Interface Vibrational Modes in GaAs-AlAs Superlattices

A. K. Sood,[a] J. Menéndez, M. Cardona, and K. Ploog
Max-Planck-Institut für Festkörperforschung, D-7000 Stuttgart 80, Federal Republic of Germany
(Received 19 February 1985)

We report the observation of interface phonons by Raman scattering from GaAs-AlAs superlattices. These modes have frequencies close to the optical phonons of bulk GaAs and AlAs and resonate strongly for laser energies near the confined exciton levels of the GaAs quantum wells. The results are analyzed in terms of an electrostatic continuum model. In the long-wavelength limit this theory predicts the phonons of the layered media proposed by Merlin *et al.*

PACS numbers: 63.20.Dj, 73.40.Lq, 78.30.Gt, 78.40.Fy

The new periodicity along the z axis affects the acoustical and optical phonon branches of a semiconductor superlattice in qualitatively different ways.[1-5] While the acoustical branches of the constituent materials always overlap, leading to propagation of vibrations and showing the phenomenon of folding, the optical phonon branches can be separated in energy. If this occurs, the modes cannot propagate and become confined in either slab. This is the case in GaAs-AlAs superlattices. This phenomenon is very often quoted as "folding" of the optical branches,[5,6] although it is more appropriately described by the concept of confinement (as in the electronic problem).[4] The folding of the acoustic branch was first demonstrated in Ref. 4. For the optical modes, early Raman investigations[2,7] were not conclusive. In fact, Merlin *et al.*[6] explained new structures observed in the Raman spectra[6,7] without invoking the confinement argument. They showed that the optical anisotropy induced by the boundary conditions at the interfaces can modify the phonon frequencies.[6] Very recent work, however, has brought strong evidence for the confinement of the LO and TO branches.[5,8,9]

Nevertheless, the very existence of confined optical phonons does not invalidate the model of Ref. 6, which was based on very general dielectric properties of layered materials, independent of the details of the phonon structure of the superlattice. Thus, the question arises as to what is the nature of the vibrations proposed by Merlin *et al.* and what is their connection with the recently discovered confined optical phonons.

In this paper, we present Raman results obtained for GaAs-AlAs superlattices of short period, for which the effect of confinement of the optical branches is clearly seen. Together with the confined phonons, however, we observe new structures near the GaAs *and* AlAs optical frequencies which resonant strongly with the excitons *localized in the GaAs quantum wells.* This structure is assigned to interface vibrational modes, similar to those discussed by Fuchs and Kliewer,[10] and recently by Lassnig.[11] The frequency and dispersion of these modes can be analyzed in terms of an electrostatic model[10-13] which yields reasonable agreement with our results. On the other hand, the theoretical expression deduced for the dispersion relations is of interest because, in the long-wavelength limit, it reduces to the conditions found by Merlin *et al.* Thus, the anisotropic phonons of Ref. 6 are actually the long-wavelength limit of the interface vibrations in superlattices. The nature of the interface modes, however, is quite different from that proposed by Merlin *et al.* who attributed their peaks near the LO frequency of GaAs to LO phonons of B_2 and E symmetry in the superlattice (point group D_{2d}).

Raman experiments were performed at ~ 10 K for three [001]-oriented GaAs-AlAs superlattices in the backscattering configuration. The sample parameters are $d_1 = 20$ Å, $d_2 = 20$ Å (sample A); $d_1 = 20$ Å, $d_2 = 60$ Å (sample B); $d_1 = 60$ Å, $d_2 = 20$ Å (sample C), where d_1 and d_2 are the thicknesses of the GaAs and AlAs layers, respectively. The period $d = d_1 + d_2$ was repeated 400 times for samples A and B and 100 times for sample C. Raman spectra were excited with a cw dye laser pumped with an Ar^+ laser. DCM (Spectra Physics) was used as a dye. Nonresonant Raman spectra were taken with the green (5145 Å) line of the pump laser. The scattered light was analyzed with a 1-m Jarrell Ash double monochromator and detected by photon counting.

Figure 1 shows typical spectra for samples A and B in the region of the GaAs optical modes, taken for the scattered light ω_S in resonance with ω_1, the first electron–heavy-hole exciton in the GaAs quantum wells. The spectra are shown for $z(x,x)\bar{z}$ scattering configuration. A similar (weaker) spectra is obtained for $z(x,y)\bar{z}$ configuration (x,y,z are the crystal axes, and z is the superlattice axis). The series of peaks labeled LO_m correspond to confined LO phonons of A_1 symmetry in the D_{2d} point group of the superlattice. The energy of these phonons is given by $\Omega_m = \Omega(m\pi/d_1)$, where $\Omega(q)$ is the dispersion of the LO branch along the [001] direction in bulk GaAs. Confined phonons of B_2 symmetry (m odd) are only seen far from resonance. This phenomenon is discussed elsewhere.[9] The confined phonons in samples A and B have the same energy because the parameter d_1 is the same. However, the peak on the high-energy side of LO_6, labeled IF, has a relative shift in sample B

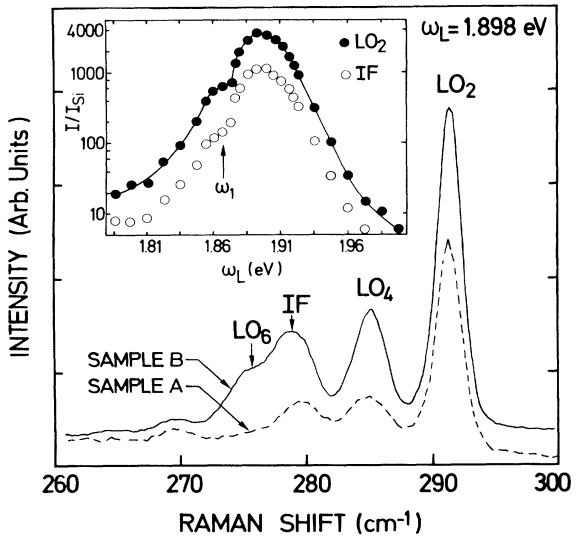

FIG. 1. Raman spectra for samples A and B in $z(x,x)\bar{z}$ scattering configuration ($x=[100]$, $z=[001]$). The peaks labeled LO_m are the confined LO phonons and IF corresponds to the GaAs-like interface mode. The inset shows the resonant behavior of LO_2 and the IF mode, the intensities measured with respect to the Raman phonon of Si.

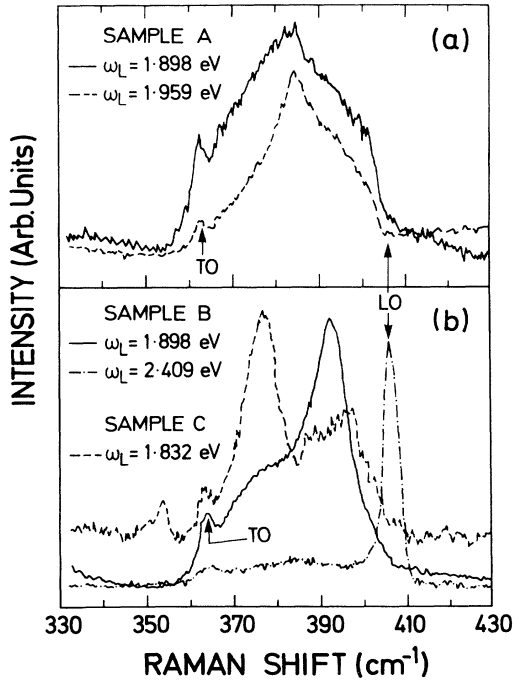

FIG. 2. AlAs-like interface modes for samples A, B, and C. All spectra correspond to the $z(x,x)\bar{z}$ scattering configuration.

with respect to sample A. Moreover, LO_6 and IF cannot be simultaneously fitted with any reasonable $\Omega(q)$ function if it is assumed that both represent confined LO phonons. We assign IF to an interface vibration. Whereas the confined phonons are localized in their corresponding ionic slabs, for an interface mode the vibrational amplitude is different from zero in both materials.

The effect can be more clearly seen in the region of AlAs-like vibrations, shown in Fig. 2. Here the off-resonance spectrum presents the usual AlAs-like LO phonon (shown only for sample B). When the laser resonates with the first exciton in GaAs, however, the spectra are dominated by broad structures below that peak. These structures have a different shape for samples A, B, and C. They cannot be attributed to folded AlAs phonons, not only because of their shape, but also because folded AlAs phonons should be *localized* in the AlAs slabs. Thus, coupling with the excitons confined in the GaAs quantum wells cannot take place. The fact that the Raman structure corresponding to these vibrations resonates at the GaAs exciton implies that they produce some long-range electric field in the GaAs slabs.

We attribute the novel structures we observe to interface phonons in the superlattice. These modes correspond to the surface vibrations discussed by Fuchs and Kliewer[10] for isolated ionic slabs. Their coupling with the electronic system has been theoretically investigated.[12,13] The theory has been extended to double heterostructures,[11] and to superlattices.[14] It is based on an electrostatic analysis, whereby one looks for solutions of the macroscopic Maxwell equations. For a superlattice, the dispersion of the interface modes (with neglect of retardation effects[8]) is given in implicit form by[14]

$$\cos(k_z d)=[(\eta^2+1)/2\eta]\sinh(k_x d_1)\sinh(k_x d_2)+\cosh(k_x d_1)\cosh(k_x d_2), \quad (1)$$

where $\eta=\epsilon_1(\omega)/\epsilon_2(\omega)$. Here $\epsilon_1(\omega)$ [$\epsilon_2(\omega)$] is the frequency-dependent dielectric constant of GaAs (AlAs). The phonon wave vector along the superlattice axis is given by k_z, while k_x represents the component in the plane of the slabs. The mode frequencies can be obtained from Eq. (1) by replacement

$$\epsilon_{1,2}(\omega)=\epsilon_{1,2}^{\infty}(\omega^2-L_{1,2}^2)/(\omega^2-T_{1,2}^2),$$

where L (T) indicates the LO (TO) phonon frequency in either material. This leads to an equation of fourth order in ω, which gives four solutions for each value of $\mathbf{k}$, two AlAs-like and two GaAs-like modes. The modes create a macroscopic potential, which has a symmetric and an antisymmetric component with respect to the center of the GaAs slab. For $k_z d \to 0$ and $d_1 < d_2$, the low- (high-) energy GaAs-like mode

and the high- (low-) energy AlAs-like mode are mostly symmetric (antisymmetric). These symmetry properties are reversed for $d_1 > d_2$: For instance, the low-energy GaAs-like modes become mainly antisymmetric, etc. For $d_1 = d_2$ and $k_z d \to 0$ the symmetric and antisymmetric potential components are equal. The effect of a larger k_z is to make the higher- (lower-) energy GaAs (AlAs) modes more asymmetric and the lower- (higher-) energy GaAs (AlAs) modes more symmetric.

In a backscattering experiment, we expect to see interface vibrations with $k_x = 0$ and k_z given by the momentum transfer between the incident and scattered photons. However, if the scattering process is induced by impurities or interface defects, phonons of all **k** vectors can become allowed. In fact, there are strong indications that impurity-induced scattering is dominant: The resonance curve for the interface modes (inset to Fig. 1) and for the confined LO modes[9] show a maximum for the outgoing channel. This asymmetry between incoming and outgoing channels is typical for impurity-induced scattering in bulk materials,[15] due to double resonance effects.[16] If all **k** values become allowed, the solutions of Eq. (1) form bands given by the shaded areas in Fig. 3. The bands are separated by a "gap," which disappears for $d_1 = d_2$. Figure 3 shows the calculated frequencies for samples *A* and *B*. The frequencies for sample *C* can be obtained from Figs. 3(b) and 3(d) if the abscissa is taken to be $k_x d_2$ instead of $k_x d_1$; the symmetries for $k_z d \to 0$ must also be reversed.

The frequencies predicted in Fig. 3 compare well with our experimental results. On the AlAs-like vibrational region, sample *A* has a maximum midway between LO and TO [in the middle of the shaded area in Fig. 3(a)], while samples *B* and *C* cannot have their maxima there because this frequency corresponds to the "gap" in Fig. 3(b). Instead, samples *B* and *C* show an asymmetric profile [Fig. 2(b)]. The maximum in sample *B* is shifted towards the LO frequency while that of sample *C* is shifted towards the TO side. On the GaAs-like side, we see in sample *B* a well-resolved structure IF near LO_6 (Fig. 1). This structure corresponds to the low-energy side of the shaded area in Fig. 3(d). No clear indication of the high-energy GaAs-like interface modes is seen in sample *B*, but there is an indication of such structure for sample *C* (not shown in the figures).

These facts can be explained in terms of the coupling of the observed modes with the excitons via the Fröhlich electron-phonon interaction. Because the electronic wave function is symmetric with respect to the bisector plane of the GaAs-quantum well, the intraband matrix elements of the Fröhlich interaction (which produce the most strongly resonating contribution to the Raman efficiency[9]) cancel for an antisymmetric potential. Thus the low-energy GaAs-like modes and the high-energy AlAs-like modes couple stronger in sample *B*. Conversely, the high-energy GaAs-like modes and the low-energy AlAs-like modes couple stronger for sample *C*. In the case of $d_1 = d_2$ (sample *A*), we expect instead the more symmetric result seen in Fig. 2(a). In this manner we can also understand why the GaAs-like IF of sample *A* (~ 280 cm^{-1}) falls slightly below the center frequency of Fig. 3(c) since the modes become also more symmetric at these frequencies. The corresponding opposite effect for the AlAs-like IF of sample *A* is apparent in the line shape of Fig. 2(a).

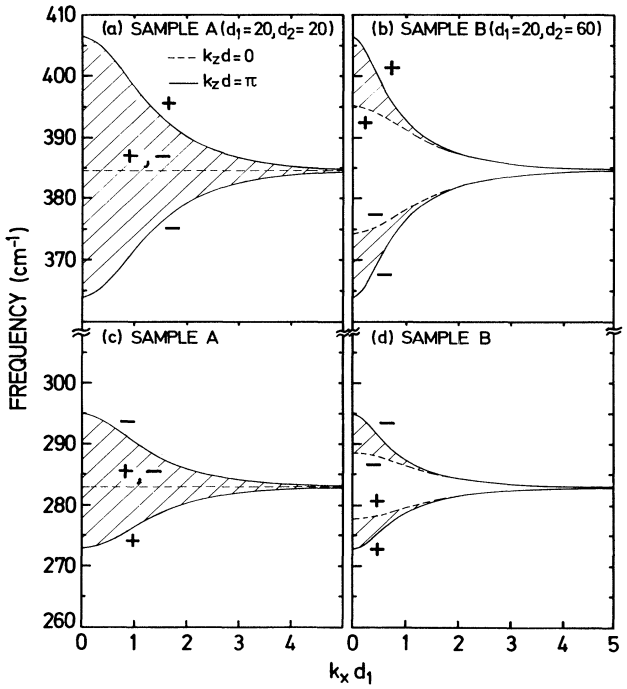

FIG. 3. Calculated interface modes from Eq. (1). The allowed frequencies form bands between the curves for $k_z d = \pi$ (solid curves) and $k_z d = 0$ (dashed curves). (a) AlAs-like modes, sample *A*; (b) AlAs-like modes, sample *B*; (c) GaAs-like modes, sample *A*; (d) GaAs-like modes, sample *B*. Plusses and minuses indicate the parity of the electrostatic potential with respect to the center of the GaAs layers.

Let us now examine some limiting cases of Eq. (1). For $k_z \to 0$, Eq. (1) splits into the following:

$$\eta = -\tanh\left(\frac{k_x d_1}{2}\right)\coth\left(\frac{k_x d_2}{2}\right), \tag{2a}$$

$$\eta = -\tanh\left(\frac{k_x d_2}{2}\right)\coth\left(\frac{k_x d_1}{2}\right). \tag{2b}$$

In the limit $k_x \to 0$, Eq. (2a) gives $\epsilon_1 d_2 + \epsilon_2 d_1 = 0$, and Eq. (2b) $\epsilon_1 d_1 + \epsilon_2 d_2 = 0$. These equations are identical

to those defining the frequencies of the modes in the layered medium in Ref. 6. Thus, the modes proposed by Merlin *et al.*[6] are the long-wavelength limit of the interface vibrations in superlattices. In Ref. 6, the long-wavelength limit of Eq. (2a) was assigned to a TO phonon of B_2 symmetry, while that of Eq. (2b) was assigned to an LO vibration of E symmetry. This assignment is not correct: The vibrations in an ionic slab have the remarkable property that all B_2 modes (z polarized) have the LO frequency and all the E modes (x polarized) have TO frequency.[11,17] This fact was experimentally demonstrated in Ref. 8. The reason for this behavior is that the effect of the superlattice periodicity on the GaAs modes is equivalent to considering that they are bulk phonons with a wave vector in the z direction given by $m\pi/d_1$. Thus, vibrations polarized along x are of TO character, regardless of the direction of the wave vector added by the impurity scattering, unless it becomes comparable to $m\pi/d_1$. Conversely, all z-polarized vibrations are LO like. Hence, the assumption of long-wavelength phonons by Merlin *et al.* is not compatible with their symmetry assignment.

So far, we have discussed our interface modes in terms of an electrostatic model. In a microscopic lattice-dynamical calculation, some other features appear.[17,18] First, one one finds new surface (interface) microscopic modes which arise from the change in the force constants near the interface. Second, the "electrostatic" interface modes interact with "bulk" vibrations of the same symmetry, yielding a much more complicated picture of the dispersion relations.[18] However, in the exact calculation for thin ionic slabs,[18] the "electrostatic" modes are shown to be a kind of "envelope function indicating for which k_x values the 'bulk' modes of the slabs" tend to be localized at the surface. We thus believe that our estimated frequencies in terms of Eq. (1) are meaningful. Furthermore, we can rule out scattering by additional "microscopic" surface modes because the frequency of these modes, which are extremely localized at the interface, should not be substantially affected by changes in d_1 and d_2, as it occurs in the experiments (Figs. 1 and 2). On the other hand, their coupling with the electronic wave functions, which extend all over the slab, is expected to be much smaller than for the electrostatic interface modes.

Despite the good qualitative agreeement between the electrostatic approximation and the observed Raman data, the need for microscopic lattice-dynamical calculations for the superlattices should be emphasized. Up to now, only results for $k_x = 0$ have been presented.[3,17] However, in order to understand the interaction between interface and bulk (folded) modes and the details of the Raman spectra, the k_x dependence of the interface modes must be investigated.

We gratefully acknowledge the technical assistance of P. Wurster, H. Hirt, and M. Siemers and thank A. Fisher for help in growing the superlattices.

---

[a]On leave from Materials Science Laboratory, Reactor Research Center, Kalpakkam-603102, India.

[1]R. Tsu and S. S. Jha, Appl. Phys. Lett. **20**, 16 (1972).

[2]A. S. Barker, Jr., J. L. Merz, and A. C. Gossard, Phys. Rev. B **17**, 3181 (1978).

[3]S. K. Yip and Y. C. Chang, Phys. Rev. B **30**, 7037 (1984).

[4]C. Colvard, R. Merlin, M. V. Klein, and A. C. Gossard, Phys. Rev. Lett. **45**, 298 (1980); C. Colvard, T. A. Grant, M. V. Klein, R. Fischer, H. Morkoc, and A. C. Gossard, Phys. Rev. B **31**, 2080 (1985).

[5]B. Jusserand, D. Paquet, and A. Regreny, Phys. Rev. B **30**, 6245 (1984).

[6]R. Merlin, C. Colvard, M. V. Klein, H. Morkoc, A. Y. Cho, and A. C. Gossard, Appl. Phys. Lett. **36**, 43 (1980).

[7]G. A. Sai-Halasz, A. Pinczuk, P. Y. Yu, and L. Esaki, Solid State Commun. **25**, 381 (1978).

[8]J. E. Zucker, A. Pinczuk, D. S. Chemla, A. Gossard, and W. Wiegmann, Phys. Rev. Lett. **53**, 1280 (1984).

[9]A. K. Sood, J. Menéndez, M. Cardona, and K. Ploog, preceding Letter [Phys. Rev. Lett. **54**, 2111 (1985)].

[10]R. Fuchs and K. L. Kliewer, Phys. Rev. **140**, A2076 (1965).

[11]R. Lassnig, Phys. Rev. B **30**, 7132 (1984).

[12]A. A. Lucas, E. Kartheuser, and R. G. Badro, Solid State Commun. **8**, 1075 (1970).

[13]J. L. Licari and R. Evrard, Phys. Rev. B **15**, 2254 (1977).

[14]E. P. Pokatilov and S. I. Beril, Phys. Status Solidi (b) **110**, K75 (1982), and **118**, 567 (1983); R. E. Camley and D. L. Mills, Phys. Rev. B **29**, 1695 (1984).

[15]J. Menéndez and M. Cardona, Phys. Rev. B **31**, 3696 (1985).

[16]R. M. Martin, Phys. Rev. B **10**, 2620 (1974).

[17]G. Kanellis, J. F. Morhange, and M. Balkanski, Phys. Rev. B **28**, 3406 (1983).

[18]W. E. Jones and R. Fuchs, Phys. Rev. B **4**, 3581 (1971).